

Semi-physical Neural Network Model in Detecting Engine Transient Faults using the Local Approach^{*}

Xun Wang^{*} Neil McDowell^{**} Uwe Kruger^{***}
Geoff McCullough^{****} George W. Irwin[†]

^{*} *Intelligent Systems and Control Research Group, Queen's University
Belfast, BT9 5AH, U.K. (e-mail: x.wang@ee.qub.ac.uk).*

^{**} *Internal Combustion Engines Research Group, Queen's University
Belfast, BT9 5AH, U.K. (e-mail: n.mcdowell@qub.ac.uk)*

^{***} *Department of Electrical Engineering, The Petroleum Institute, PO
Box 2533, Abu Dhabi, UAE. (e-mail: ukruger@pi.ac.ae)*

^{****} *Internal Combustion Engines Research Group, Queen's University
Belfast, BT9 5AH, U.K. (e-mail: g.mccullough@qub.ac.uk)*

[†] *Intelligent Systems and Control Research Group, Queen's University
Belfast, BT9 5AH, U.K. (Tel: +44(0)2890974058; e-mail:
g.irwin@qub.ac.uk)*

Abstract: This paper investigates detection of an air leak fault in the intake manifold subsystem of an automotive engine during transient operation. Previously, it was shown that integrating the local approach with an auto-associative neural network model of the engine, significantly increased the sensitivity of fault detection. However, the drawback then is that the computational load is naturally dependent on the network complexity. This paper proposes the use of the available physical models to pre-process the original signals prior to model building for fault detection. This not only extracts existing relationships among the variables, but also helps in reducing the number of variables to be modelled and the related model complexity. The benefits of this improvement are demonstrated by practical application to a modern spark ignition 1.8 litre Nissan petrol engine. *Copyright ©2008 IFAC*

Keywords: Automotive, Statistical process control, Nonlinear models, Neural networks, Fault detection, Normal distribution

1. INTRODUCTION

Due to the increased complexity of modern automotive engines, an accurate and complete physical model is rarely available. A number of techniques for Fault Detection and Diagnosis (FDD) applied to automotive engines have been published over the last decade (Gertler *et al.*, 1993; Nyberg, 2002; Crossman, 2003; Kimmich *et al.*, 2005). These include both signal-processing and model-based approaches. It has been argued that simple signal-based techniques will probably no longer be able to match the ever-rising requirements on future automotive FDD systems, leaving model-based fault detection as the most promising way forward (Kimmich *et al.*, 2005).

This paper focuses on modelling and fault detection for the intake system of a petrol engine during *transient* operation. Nyberg (2002) constructed a model-based diagnosis system for the air-intake system of a turbo-charged engine. A mean value model of the air-intake system was used. Taking into account a variety of sensor faults and leakages, different types of fault models were used within one com-

mon diagnostic system. Kimmich *et al.* (2005) have also modelled the intake system within an entire engine model structure. Physical models, in the time and angle domains, were used to describe any known relationships, with the remaining unknown ones modelled by neural networks.

Our previous work has proposed the use of a special type of neural network, the Auto-Associative Neural Network (AANN), for detecting and diagnosing different diesel engine faults (Antory *et al.*, 2005). This neural network was chosen because of its close link to Principal Component Analysis (PCA), a Multivariate Statistical Process Control (MSPC) technique. More recent work, however, showed that some faults falling within certain operating regions remained undetectable by applying the conventional Q statistic or squared prediction error. More recently we proposed integrating the local approach (Basseville, 1998) into the AANN structure, which significantly enhanced fault detection sensitivity (Wang *et al.*, 2006). In this case, an additional statistic is generated by the local approach which focuses on changes in the model parameters when the operating condition varies. Although this statistic is indeed more sensitive than the conventional one in fault detection, the computation required depends heavily on the size and complexity of the

^{*} The authors would like to acknowledge financial support from the U.K. Engineering and Physical Science Research Council (Grant No. EP/C005457).

neural network. Since the AANN has a complex structure of 5 layers, it is not only difficult to train when the number of variables increases, but also the computational load for the local approach increases dramatically. This would then be a major concern for practical implementation within the engine management system. This paper proposes the use of physical models to pre-process the engine signals before modelling. This reduces the number of variables to be modelled by the AANN, with a consequent reduction in the computational load for the local approach. The physical models also contribute to describing the relationships between the original engine variables, which removes part of the modelling from the AANN.

The complete new approach is applied to transient experimental data collected from a 1.8 litre Nissan petrol engine within a test cell, to be described in the next section. The techniques involved are outlined in Section 3, followed by application results in Section 4. The paper ends with Conclusions.

2. AUTOMOTIVE ENGINE DESCRIPTION

The target application was a 1.8 litre modern spark ignition petrol engine, manufactured by Nissan. This represents current engine technology with such devices as variable valve timing, inlet swirl plates, exhaust gas recirculation and a close coupled catalyst. The engine was installed onto a state-of-the-art engine testcell facility at Queen's University Belfast. An AC dynamometer with a Ricardo S3000 controller was used to control the engine throughout the various modes of operation. Sensor signals were recorded using the testcell data acquisition hardware – a Ricardo TaskMaster 500/2000 system, capable of recording upto 32 analogue input channels simultaneously. The engine installation can be seen in Figure 1.

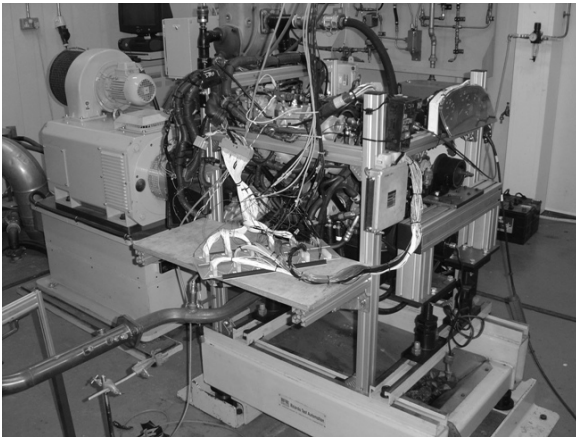


Fig. 1. Engine testcell installation

The intake subsystem of this engine was investigated. In order to simplify the air intake model, the exhaust gas recirculation (EGR) function was disabled. The following 5 variables were used here to analyze this subsystem: rotational speed (rev/min), pedal position (%), air flow (kg/h), inlet manifold pressure (bar), and inlet manifold temperature ($^{\circ}C$). Rotational speed and pedal position were the engine inputs, and were varied to generate suitable data sequences for nonlinear, dynamical modelling as in Kimmich *et al.* (2005). The remaining 3 variables

represent the behaviour of the intake system. Note that these 5 variables are all available for predetermined routine maintenance schedules, for example for the annual Ministry of Transport test in the UK.

In this investigation, the air leakage was achieved by drilling a hole of 4mm diameter into a bolt which was subsequently screwed into the inlet manifold of the engine after the throttle plate. The fault-free condition was achieved by using a solid bolt. This air leakage fault in the engine manifold can be difficult to detect under certain operating conditions. A minor air leak may potentially be unnoticeable to the driver. Nevertheless, when a fault of this type occurs, the driver would depress the throttle pedal further, until the desired speed is achieved. Thus, in this fault scenario it is imperative to preserve the values of the engine inputs i.e. the engine speed and pedal position between the fault-free and faulty conditions. The data sequences for the two manipulated variables and the corresponding engine response variables are plotted in Figures 2 and 3 respectively.

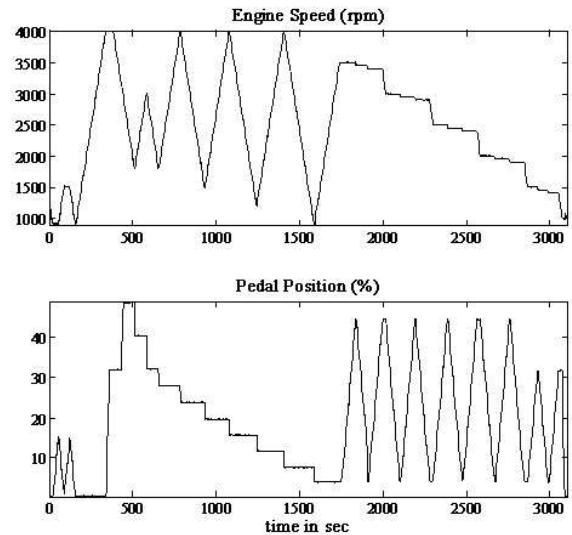


Fig. 2. Engine input signals

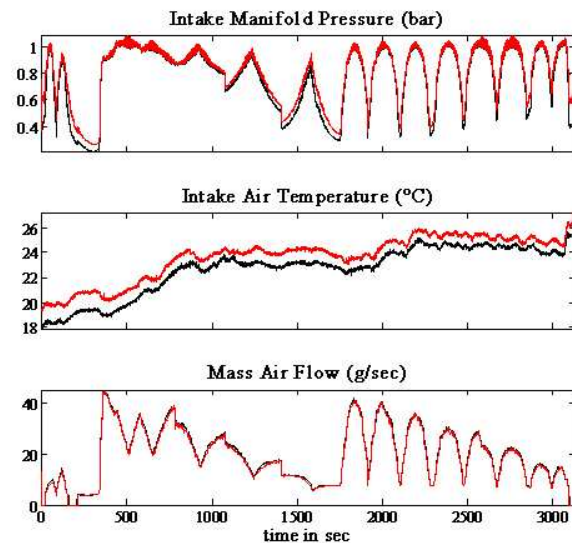


Fig. 3. Engine response signals

Three sets of data were recorded by running the same sequences of the two manipulated variables. This generated data sets for training, validation and fault detection respectively. The first two data sets are fault-free and the engine response signals are shown in Figure 3 by the black trace. The third data set incorporates the air leak fault, resulting in the different engine responses given by the red trace in Figure 3. Each data set contained 6500 samples, recorded at a sampling rate of 2Hz. Comparing the graphs for the fault-free and faulty response variables, it is clear that the intake manifold pressure and the intake air temperature exhibit the most obvious deviations.

3. INTEGRATION OF SEMI-PHYSICAL AANN WITH THE LOCAL APPROACH

3.1 Available physical models for intake system

The theoretical air mass flow into the engine can be represented by the following physical model, describing the engine pumping corresponding to an ideal positive-displacement pump.

$$\dot{m}_{air,th} = \frac{1}{2}n_e V_d \rho_{2,i} \quad (1)$$

where $\dot{m}_{air,th}$ is the theoretical air flow, V_d is the engine displacement volume, and n_e is the engine speed. Note that the measured mass air flow is denoted by $\dot{m}_{air,e}$ and $\rho_{2,i}$ is the inlet manifold air density:

$$\rho_{2,i} = \frac{p_{2,i}}{RT_{2,i}} \quad (2)$$

where $p_{2,i}$ and $T_{2,i}$ are inlet manifold pressure and temperature respectively, and R is the individual gas constant. These physical models are integrated into the AANN as shown in Figure 4.

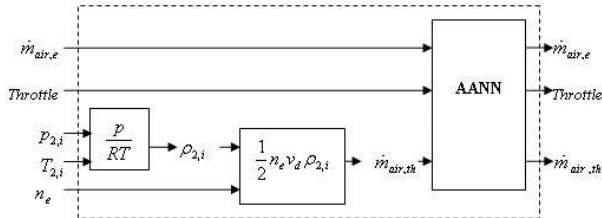


Fig. 4. Structure of semi-physical system

All the 5 measured signals from the engine are used as inputs to the AANN. Note that by introducing two simple physical models, the three variables, $p_{2,i}$, $T_{2,i}$, and n_e , are now combined into one, viz. $\dot{m}_{air,th}$. Only 3 variables now have to be modelled by the AANN, as explained in the next subsection.

3.2 Autoassociative neural network model

This nonlinear, dynamic neural model has the architecture shown in Figure 5.

The AANN represents an identity mapping for a given set of n variables, denoted in Figure 5 by the vector $\mathbf{x}^T = (x_1 \cdots x_n)$, such that the input and output variables are regarded as representing the nonlinear scores t_1, \dots, t_i of a nonlinear PCA model. The activation functions used in

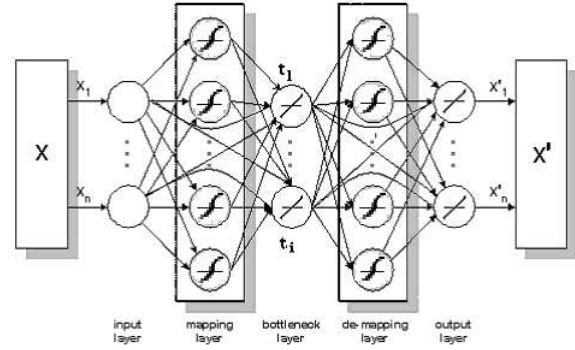


Fig. 5. Autoassociative neural network architecture

the mapping and demapping layers are hyperbolic tans of the form $\psi(\cdot) = \frac{2}{1+\exp(-2\cdot)} - 1$. The bottleneck and output layers have linear activation functions. It should also be noted that there are direct links from inputs to the scores and from the scores to the outputs.

This neural network was used for modelling the 3 variables shown in Figure 4, viz. $\dot{m}_{air,e}$, $\dot{m}_{air,th}$, and throttle position. Once the model had been properly trained and validated, the local approach was introduced to provide the Hotelling's T^2 statistic needed for fault detection.

3.3 Applying the local approach to the AANN

A detailed explanation of generating the Hotelling's T^2 statistic using the local approach applied to an AANN was given in earlier papers (Wang *et al.*, 2006; Wang *et al.*, 2007). Here only the key steps leading to the resulting statistic are presented.

First \mathcal{Q} is defined as the matrix containing all the parameters (weights and bias terms) of the AANN model, and \mathcal{Q}_0 corresponds to the normal operating conditions. The derivatives of the cost $J_k(\mathcal{Q}) = \|\mathbf{x}(k) - \mathbf{x}'(k)\|_2^2$ with respect to \mathcal{Q} for the k th sample, results in the following condition if the process is in "normal" operating mode:

$$E \left\{ \nabla(J_k) |_{\mathcal{Q}=\mathcal{Q}_0} \right\} = \mathbf{0}, \quad (3)$$

where $\nabla(\cdot)$ is the gradient vector of partial derivatives of J_k with respect to \mathcal{Q} .

Using the above derivatives, an improved residual vector $\mathcal{Z}(\nabla(J), k)$ is defined as:

$$\mathcal{Z}(\nabla(J), k) \triangleq \frac{1}{\sqrt{k}} \sum_{j=1}^k \frac{\partial \|\mathbf{x}(j) - \mathbf{x}'(j)\|_2^2}{\partial \mathcal{Q}} \Bigg|_{\mathcal{Q}=\mathcal{Q}_0} \quad (4)$$

Using this definition of $\mathcal{Z}(\nabla(J), k)$, a Hotelling's T^2 statistic is then calculated as follows:

$$T^2(\mathcal{Z}, k) = \mathcal{Z}^T(\nabla(J), k) \Sigma^{-1}(\mathcal{Q}_0) \mathcal{Z}(\nabla(J), k), \quad (5)$$

with the null and alternative hypothesis tests being formulated as:

$$H_0 : T^2(\mathcal{Z}, k) \leq T_0^2 \quad H_1 : T^2(\mathcal{Z}, k) > T_0^2, \quad (6)$$

where T_0^2 is the 95% (or 99%) confidence limit for a χ^2 distribution function for which the number of degrees of freedom equals to the dimension of $\mathcal{Z}(\cdot)$.

Obviously the sensitivity in detecting changes in the mean value of $\mathcal{Z}(\cdot)$ reduces as k is ever-increasing. However, it

has been suggested in (Zhang *et al.*, 1994) that this can be handled by using a moving window such that:

$$\mathcal{Z}(\nabla(J), k) \triangleq \frac{1}{\sqrt{k_0}} \sum_{j=k-k_0+1}^k \frac{\partial \|\mathbf{x}(j) - \mathbf{x}'(j)\|_2^2}{\partial \mathcal{Q}} \Bigg|_{\mathcal{Q}=\mathcal{Q}_0}, \quad (7)$$

where k_0 is the window length. Typically there is a tradeoff involved in the selection of k_0 : a larger k_0 may reduce the number of false alarms, but it also reduces the sensitivity of $\mathcal{Z}(\cdot)$ in detecting incipient faults. In practice, k_0 should be selected according to the performance of Hotelling's T^2 statistic on faulty and validation data. Its value must be small enough to produce the necessary sensitivity for fault detection, and also be sufficiently large so that the validation data does not produce too many false alarms.

3.4 Overall system for fault detection

The proposed overall system for fault detection using dynamical engine data is shown in Figure 6. It is worth noting that this approach is generally applicable. The physical models are used to process the engine signals, reducing the number of variables to be modelled from 5 to 3. An AANN model is then built from experimental data relating to these 3 variables. The Q statistic is directly calculated from the trained neural network model as the squared prediction error. When the local approach is applied to this AANN model, the improved residual vectors are calculated to produce the Hotelling's T^2 statistic.

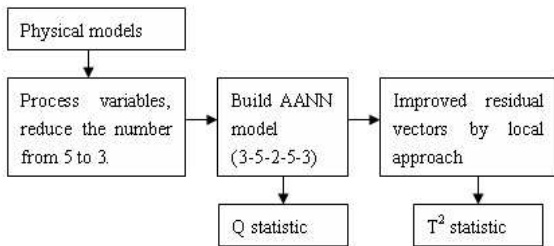


Fig. 6. Overall scheme for fault detection

The Q and Hotelling's T^2 statistics are now used for detecting the engine fault as detailed in the next section.

4. ENGINE APPLICATION STUDY

All 3 sets of engine data were pre-processed using the physical models, reducing the number of variables from 5 to 3. In the absence of pre-processing using the physical models, a 5-15-3-15-5 AANN was required to produce a satisfactory modelling accuracy. By contrast, the new semi-physical model had a much simpler structure in the form of a 3-5-2-5-3 AANN. The monitoring charts shown in this section include all the three data sets. The statistics generated from the training data are used for calculating the 95% and 99% confidence limits. The validation data was employed to double check the reliability of the AANN model. If the Q statistic calculated from the validation data exceeded the confidence limits, then the model could have been over-fitted to the training data. Generating the Hotelling's T^2 statistic for the validation data helped in selecting an appropriate window size for the local approach.

Figure 7 shows the Q statistic for all 3 data sets, which are shown separated by vertical lines. Its values are almost identical for the training and validation data sets, because both were collected under fault-free conditions. Unfortunately, although the third data set contains the fault, the Q statistic is not sensitive enough to detect it.

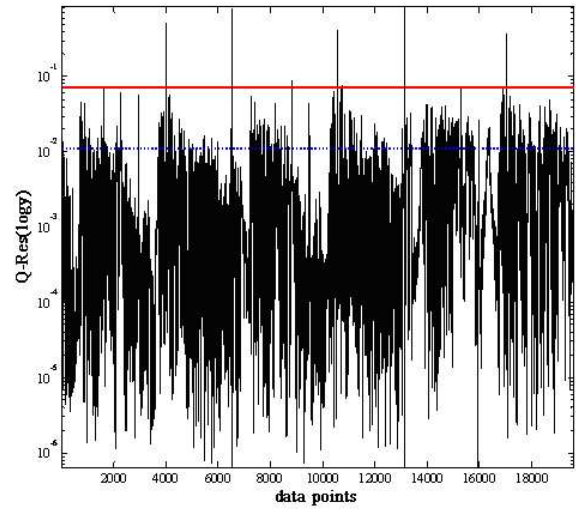


Fig. 7. Q statistic from semi-physical AANN model applied to fault detection

For the local approach, the window size was chosen as 10 using trial-and-error by observing the T^2 statistic values across the validation and faulty data sets. The T^2 statistic arising from the local approach is able to detect the engine fault, as seen in Figure 8. Note that there are certain regions in the faulty data where effect of the air-leak is not apparent. This is expected, as the fault would not affect the engine when it has high throttle openings. Under such circumstances, the manifold pressure is close to, or equal to, the atmospheric pressure. Consequently, not much air would pass through the leakage hole because the pressure difference would be negligible.

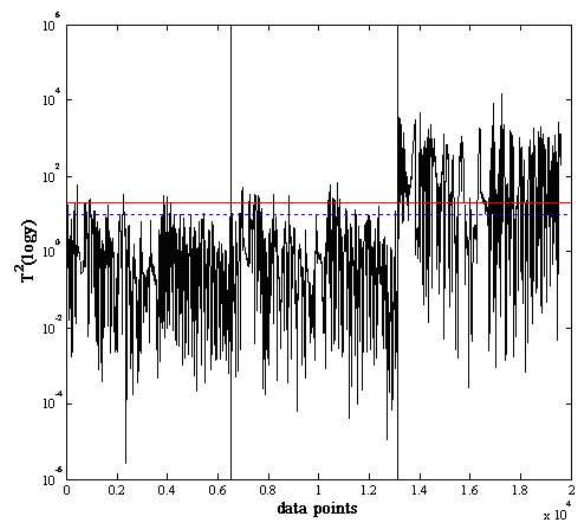


Fig. 8. Hotelling's T^2 statistic applied to engine fault detection based on an AANN

The advantage of introducing the local approach to the AANN is, once again, an enhanced sensitivity for fault

detection, as suggested in a previous simulation study (Wang *et al.*, 2006) and by application to a diesel engine (Wang *et al.*, 2007). Further, by using the physical models to reduce the number of variables to be modelled, the computational load is greatly eased. If the original 5-15-3-15-5 for all the original variables was used, there would be a total of 305 improved residual vectors needed for applying the local approach. The semi-physical model used to produce the results shown in Figure 8 (3-5-2-5-3) allowed this number to be reduced to 75.

5. CONCLUSIONS

This paper proposed a modified modelling and fault detection approach for an automotive engine intake system. It combined three elements, namely the physical models, an AANN, and the local approach. Physical models helped in reducing the complexity of the AANN model by capturing a priori known information about the engine signals. It also significantly eased the computational load involved in the local approach. The local approach provided an additional T^2 monitoring statistic for fault detection, which proved to be more sensitive than the conventional Q one. Application to dynamic experimental data from a 1.8 litre Nissan petrol engine verified these benefits.

REFERENCES

- J.J. Gertler, M. Costin, X. Fang, R. Hira, Z. Kowalczyk, and Q. Luo. Model-Based On-Board Fault Detection and Diagnosis for Automotive Engines. *Control Engineering Practice*, 1(1), pages 3–17, 1993.
- M. Nyberg. Model-Based Diagnosis of an Automotive Engine Using Several Types of Fault Modes. *IEEE Transactions on Control Systems Technology*, 10(5), pages 679–689, 2002.
- J.A. Crossman, H. Guo, Y.L. Murphey, and J. Cardillo. Automotive Signal Fault Diagnostics - Part I: Signal Fault Analysis, Signal Segmentation, Feature Extraction and Quasi-Optimal Feature Selection. *IEEE Transactions on Vehicular Technology*, 52(4), pages 1063–1075, 2003.
- F. Kimmich, A. Schwarte, and R. Isermann. Fault Detection for Modern Diesel Engines Using Signal- and Process Model-based Methods. *Control Engineering Practice*, 13, pages 189–203, 2005.
- D. Antory, U. Kruger, G.W. Irwin and G. McCullough. Fault Diagnosis in Internal Combustion Engines Using Nonlinear Multivariate Statistics. *Proceedings of the Institution of Mechanical Engineers, Part I Journal of Systems and Control Engineering*, 219(4), pages 243–258, 2005.
- X. Wang, U. Kruger, G.W. Irwin, N. McDowell, and G. McCullough. Nonlinear PCA for Process Monitoring using the Local Approach, *Proceedings of the 6th IFAC Symposium on Fault Detection, Supervision and Safety of Technical Processes*, 30. August-01. September, Beijing, P.R. China, pages 115–120, 2006.
- X. Wang, U. Kruger, G.W. Irwin, N. McDowell, and G. McCullough. Nonlinear PCA with the Local Approach for Diesel Engine Fault Detection and Diagnosis, *IEEE Transactions on Control Systems Technology*. To appear.
- M. Basseville. On-board Component Fault Detection and Isolation Using the Statistical Local Approach. *Automatica*, 34(11), pages 1391–1415, 1998.
- Q. Zhang, M. Basseville and A. Benveniste. Early Warning of Slight Changes in Systems and Plants with Application to Condition Based Maintenance. *Automatica*, 30(1), pages 95–114, 1994.